ELSEVIER

Carbohydrate Polymers 52 (2003) 151–166

Carbohydrate Polymers

www.elsevier.com/locate/carbpol

Molecular weight effects on solution rheology of pullulan and mechanical properties of its films

Athina Lazaridou, Costas G. Biliaderis*, Vassilis Kontogiorgos

Food Science and Technology Department, Laboratory of Food Chemistry and Biochemistry, School of Agriculture, Aristotle University, Thessaloniki 54006 Greece

Accepted 23 September 2002

Abstract

The effects of molecular weight on solution rheology of pullulan, and on thermomechanichal properties of sorbitol and/or water-plasticized pullulan specimens, prepared by either hot pressing or casting of aqueous solutions, were studied. Pullulan samples differing in molecular weight were characterized by ^{13}C NMR spectroscopy and size exclusion chromatography combined with a multiangle laser light scattering and a refractive index detector. For samples with weight average molecular weight (M_w) ranging between 100 and 560×10^3, the values of limiting viscosity ([η]), critical concentration (c^*) and coil overlap parameter ($c^*[\eta]$) were within the range 0.38–0.70 dl/g, 1.4–3.1 g/dl and 1.0–1.2 dl/g, respectively. The thermomechanical properties of five molecular weight grades of pullulan, either alone or with sorbitol (plasticized at a 10% d.b. level) were examined by dynamic mechanical thermal analysis (DMTA). A large drop in storage modulus E' ($\sim 10^{1.5}$–10^3 Pa) and a peak in tan δ in the DMTA traces accompanied the glass–rubber transition (T_g) or the α-relaxation (T_α) of pullulan; the magnitude of the drop in E' and the tan δ peak height increased with increasing water content. The plasticizing action of water and sorbitol was evident in the DMTA curves, and the T_g vs. moisture content data were fitted to the Gordon–Taylor empirical model. Within the range of molecular weights tested there was no effect of polymer molecular weight on T_g. A β-relaxation detected by DMTA was shifted to lower temperature with increasing moisture content and to higher temperature with addition of sorbitol. Apparent activation energies for α-relaxation ($E_\alpha\alpha$) and β-relaxation ($E_\alpha\beta$) processes, estimated from multifrequency measurements, were within 171–640 and 118–256 kJ/mol, respectively; the values for $E_\alpha\alpha$ and 'fragility' parameter decreased with increasing moisture content. Analysis of viscoelasticity data using the time–temperature superposition principle with the Williams–Landel–Ferry equation was successful over the range T_g to $T_g + 40$ °C, provided that the coefficients C_1 and C_2 are optimized and not allowed to assume their 'universal' values. Large deformation mechanical tests demonstrated large decreases in tensile (Young's) modulus (E) and strength ($\sigma_{\max}$), and an increase in percentage elongation with increasing water content and/or addition of sorbitol in pullulan films. Relationships between the tensile parameters (E and $\sigma_{\max}$) and water content showed an increase in stiffness of the films from 3 to 7% moisture, and a strong softening effect at higher water contents. The tensile tests revealed some relationships between mechanical properties under uniaxial load and the molecular characteristics of pullulan, e.g. E, $\sigma_{\max}$, and elongation values increased with increasing molecular weight.

Keywords: Pullulan; Molecular weight; Solution rheology; Thermomechanical properties; Tensile strength; Coil overlap parameter; Glass transition; β-Relaxation; Films; Plasticizer

1. Introduction

Pullulan is an extracellular water-soluble microbial polysaccharide produced by different strains of *Aureobasidium pullulans*. It is a linear mixed linkage α-D-glucan consisting mainly of maltotriose units interconnected via α-(1 → 6) linkages. While not extensively exploited, the physical properties of this biopolymer make it suitable for a multitude of applications in the food, cosmetic, and pharmaceutical industries. The major interest in pullulan relies on its capacity to form strong resilient films and fibers. Purified pullulan can form thin films or molded products by solution casting or thermoplastic extrusion, which are biodegradable, transparent, oil resistant and impermeable to oxygen. Pullulan and its derivatives may be thus used as food coating and packaging material, as well as sizing agent

---

* Corresponding author. Tel.: +30-2310-471467; fax: +30-2310-471257.

E-mail address: biliader@agro.auth.gr (C.G. Biliaderis).

0144-8617/03/$ - see front matter © 2003 Elsevier Science Ltd. All rights reserved.
PII: S0144-8617(02)00302-8

for paper. Despite of being an α-D-glucan, pullulan is resistant to α-amylolysis and may be used in low-calorie food formulations as fat replacer. Other potential applications include use as an adhesive binder, thickener, and encapsulating agent (Deshpande, Rale, & Lynch, 1992; Hannigan, 1984; Selim, Tsimidou, & Biliaderis, 2000; Serris & Biliaderis, 2001; Yuen, 1974).

The molecular weight of pullulan is adjustable from 10^3 or lower to 10^6 or even higher by selecting the optimal strain and varying the fermentation conditions (Yuen, 1974). An approach to relate functional properties to molecular characteristics of the polysaccharide is needed as the latter are important determinants of its functionality and its end-use properties, e.g. as a food coating, packing material or encapsulating matrix (mechanical and gas barrier properties), as an adhesive (viscosity, adhesiveness, moisture-retention), and as fat mimetic in low-calorie food formulations (viscosity, dispersibility). Additionally, pullulan is an ideal model system for studying the effects of molecular size on thermal and mechanical properties, i.e. being an amorphous and linear polymer of maltotriosyl units, crystallinity and chain branching, are not factors which can complicate the thermomechanical properties of this polysaccharide. The functional properties of biopolymers in food applications are often determined primarily by whether, under hydrated conditions, they exist as disordered molecules whose interactions depend largely on space-occupancy considerations, or as ordered structures capable of stable association into long-range networks or packed aggregates (Chronakis & Kasapis, 1995). Pullulan is a typical flexible random coil polymer, exhibiting solutions with Newtonian or almost Newtonian flow behavior (at low polymer concentrations), and of relatively low viscosity, as well as pH and salt tolerance (Rees, 1977).

The structure–property relationships of hydrated biopolymers in the low-moisture content regime and their broader implications on processing and product quality can be better understood within the theoretical framework of glass transition, as frequently advocated by Slade and Levine (1991, 1993). Glass transition is a second-order phase transition (often referred to as α-relaxation) that occurs over a temperature range at which a glassy material enters the rubbery domain with a contaminant drop ($\sim 10^3$ times) in the elastic moduli (Young's or shear moduli). Changes in the mechanical properties of a polymer around T_g are of major practical interest as glasses have high moduli, i.e. they are solid, hard and brittle, and practically stable over accessible storage periods (Slade & Levine, 1991; Sperling, 1986). With temperature increasing above T_g, various physical properties are significantly affected by a consequent exponential increase in molecular mobility, decreased viscosity, and enhanced rate of physical changes (e.g. crystallization) and chemical reactivity (Slade & Levine, 1991). In a amorphous polymer the α-relaxation, as determined by thermomechanical analysis, corresponds to the glass transition and reflects motions of fairly long chain segments (long-range motions). At the rubber–glass transition the wriggling motion of long chains is frozen out, leaving the chains locked into an entangled mass and leading to limited structural reorganizations. Relaxations at lower temperatures (labeled β, γ, δ,… with decreasing transition temperature, and named as secondary relaxations) are generally due to local movements of the main chain, or rotations and vibrations of terminal groups or other side chains (short-range motions). They are assumed to occur in regions of the material where the mobility is easier, so called 'islands of mobility' or more recently 'quasi point defects' (Montes, Mazeau, & Cavaille, 1997; Simatos, Blond, & Perez, 1995). In the case of side-group motions, the relaxation process involves localized non-cooperative motions, while motions of the main chain segments are cooperative (Montes & Cavaille, 1999). The origin (intra- vs. inter-molecular effects) of the two most fundamental and recognized transitions of glassy polymers, the T_g (or T_α) and T_β (β-relaxation), are still topics of debate among scientists in this field (Ngai, Rendell, & Yee, 1988; Ngai, Rendell, Yee, & Plazek, 1991; Ngai, Roland, O'Reilly, & Sedita, 1992; Plazek & Ngai, 1991; Verghese, Jensen, Lesko, & Ward, 2001).

Besides the molecular weight and structure of a polymer the presence of a plasticizer affects the value of T_g. For example, water exerts a strong plasticizing action in hydrophilic polymers, causing a large depression of their glass transition temperature. On a molecular level, water plasticization of a polymer leads to increased intermolecular distances (free-volume), decreased local viscosity and increased back-bone chain segmental mobility (Slade & Levine, 1991). Moreover, the addition of low molecular weight plasticizers to an amorphous biopolymer has the same effect as increased temperature on molecular mobility (Slade & Levine, 1991). Thus, the addition of plasticizing agents to edible films and coatings is often required to overcome film brittleness caused by extensive intermolecular forces; the latter presupposes compatibility between polymer and the plasticizer. Plasticizers reduce interchain forces and increase the mobility of polymer chains, thereby improving flexibility and extensibility of the film. This avoids chipping or cracking of the film during subsequent handling and storage (Banker, 1966).

The aim of the present investigation was to study the effect of molecular weight on solution rheology, as well as on thermomechanical properties of pullulan under the plasticizing action of water and a polyol.

2. Materials and methods

2.1. Materials and sample preparation

Five samples of pullulan with different molecular weights were used in this work. Sample P_{360} was a commercial product (Hayashibara Biochem. Lab. Inc., Okayama, Japan) that was fractionated by a solvent-gradient technique into three different molecular mass fractions. The material was first dissolved (4% w/v) in water. Ethanol (97% v/v) was then added to the pullulan solution up to 18% (v/v) and the solution was allowed to stand overnight at 4 °C. The precipitated polysaccharide was collected by filtration, redissolved in water and freeze-dried; this fraction was designated as P_{560}. The ethanol concentration in the remaining filtrate was subsequently adjusted to 35% (v/v) and the corresponding precipitated polysaccharide fraction was designated as P_{260}. Fraction $P_{60,12}$ was received by concentration and freeze drying of the remaining filtrate, which was soluble in ethanol even after adding ethanol up to 75% (v/v). Sample designated as P_{100} was produced by *Aureobasidium pullulans* fermentation of beet molasses in a stirred tank fermentor as described by Lazaridou, Roukas, Biliaderis, and Vaikousi (2002). Sorbitol (analytically pure) was obtained from Sigma Chemical Co. (St Louis, MO, USA) and inorganic salts (reagent grade) used for adjusting the relative humidity were products of Merck KGaA (Darmstadt, Germany).

For small deformation mechanical tests (bending mode), thick specimens (1.0–1.5 mm) were obtained by hot pressing of freeze-dried pullulan powders and pullulan–sorbitol mixtures (-10S). The later were obtained by adding sorbitol (10% w/w) to pullulan solutions (7% w/v), mixing until complete solubilization and freeze drying the mixtures. Freeze dried pullulan and polyol–pullulan blends were exposed to 100% relative humidity for 24 h and hot pressed at 100 °C for 12 min at ~6 MPa. For large deformation mechanical tests (tensile mode), polysaccharide films (with thickness 0.1 ± 0.02 mm) were prepared by casting aqueous solutions. The film-forming solutions were obtained by dissolving pullulan (4% w/v) in water at 80 °C under stirring and then adding sorbitol (10% dry basis) to the solution in the case of polyol–pullulan mixed systems. All solutions were casted on plastic frames ($10 \times 10 \times 1.5$ cm^3) and dried slowly at room temperature for several days.

Hydration of both thick specimens and films at various levels of moisture was achieved by conditioning in different relative humidity chambers (saturated salt solutions). The moisture content of all samples was determined by oven drying at 130 °C for 1 h.

2.2. Molecular characterization of pullulan

Size exclusion chromatography for molecular characterization of pullulan was carried out with a high performance size exclusion chromatography (HPSEC) system which consisted of a pump (Waters 510), an injection valve (Model 7010, Rheodyne) with a 200 μl sample loop, a guard column (TSK PWH, TosoHaas GmbH, Stuttgart, Germany), a SEC column (TSK G5000 PW column, 7.8 × 600 mm, TSK PW, TosoHaas GmbH), a multiangle laser light scattering (MALLS) detector (Dawn DSP, Wyatt Technology Inc., Santa Barbara, CA) and a RI detector (Waters 410). Chromatography was performed at room temperature. The flow rate of the mobile phase (0.15M $NaNO_3$ containing 0.02% NaN_3), which was filtered through 0.2 μm and then 0.1 μm of cellulose acetate membranes, was 0.4 ml/min. Estimation of M_w, M_n and R_g was with the help of the Astra 4.72 software (Wyatt Technology); calculations were carried out with a $(dn/dc) = 0.147$ ml/g. Pullulan standards with known M_w values (P-50, M_w 47,300; P-400, M_w 404,000; P-800, M_w 788,000) were used to determine the proper experimental setup and calculations. Estimates of the polydispersity index (M_w/M_n) were also obtained. A complementary HPSEC system with similar configuration [a single pump (Marathon IV, Rigas Labs, Thessaloniki, Greece), a guard TSK PWH column and a 7.8 × 600 mm TSK G5000 PW-SEC column, and a RI detector (ERC-7515A, ERC-Inc. Nishiaoki, Kawaguchi-City, Japan)] was employed to determine the molecular size distributions of the pullulan samples; 0.15M $NaNO_3$ as mobile phase and a flow rate of 0.4 ml/min were used.

The structure and purity of the samples was also assessed by ^{13}C NMR spectroscopy. The proton-decoupled ^{13}C NMR spectra (300 Hz) were recorded on a Bruker AM 300 FT spectrometer at 70 °C, polysaccharide concentration 2% (w/v) in 50% (v/v) d6-DMSO/H_2O, 30,000 pulses with a pulse repetition time of 1.245 s, and an r.f. pulse angle 80.0°. Chemical shifts were expressed in parts per million downfield from external Me_4Si but were actually measured by reference to internal 1,4-dioxane ($\delta = 67.4$ ppm).

2.3. Solution rheological measurements

For determination of intrinsic viscosity [η], critical concentration c^* and coil overlap parameter, the viscosity of aqueous solutions of pullulan (0.02–1.5 w/v) were measured with Ubbelohde capillary viscometers at 20 °C. All measurements were taken in the Newtonian region as verified by tests with viscometers of varying capillary diameters. Steady shear viscosity measurements were also performed on a rotational Physica MCR 300 rheometer (Physica Messtechnic GmbH, Stuttgard, Germany) using a concentric cylinder (diameter of cup and bob, 28.92 and 26.66 mm, respectively) or a double gap cylindrical geometry. Aqueous solutions of pullulan (0.4–12% w/v) were subjected to shear sweeps between 1 and 1200 s^{-1} at 20 ± 0.1 °C.

2.4. Small deformation mechanical tests

The dynamic mechanical thermal analysis (DMTA) was performed on thick specimens ($\sim 2.2 \times 0.5 \times 0.2$ cm^3), conditioned at various levels of moisture content. A Mark III analyzer (Polymer Labs. Loughborough, UK) was used in the single cantilever bending mode, with a standard heating rate of 2 °C min^{-1}, at frequencies of 1, 3 and 10 Hz and a strain ×2, corresponding to a maximum displacement of 32 μm. Samples were covered with a thin layer of silicone oil to reduce moisture losses during the heating cycle.

For constructing the state diagrams, the T_g (or T_α) was determined either as the onset of storage modulus (E') drop or as the peak in tan δ ($\tan\delta = E''/E'$, where E'' and E' are the loss and storage modulus, respectively), derived from measurements at 3 Hz frequency. Data analysis to fit the experimental values of T_g to the empirical Gordon–Taylor (G–T) equation (Gordon & Taylor, 1952) was performed using the Table Curve™ software (Jandel Scientific), a non-linear least-square curve fitting package:

$$T_g = \frac{w_1 T_{g1} + k w_2 T_{g2}}{w_1 + k w_2}$$

where w_1 and w_2 are the respective weight fractions of the pullulan sample (sorbitol-plasticized or not) and water, T_{g1} is the T_g of the sample, T_{g2} is the T_g of amorphous water, and k is a constant related to the strength of polymer–diluent interactions. The constructed G–T plots were based on the best data fitting to the equation (i.e. optimization for both parameters, k and T_{g1}) of the results derived from DMTA traces; a T_g of −138 °C was used for water (Sugisaki, Suga, & Seki, 1968).

For some specimens, DMTA measurements at a variety of frequencies (0.3, 1, 2, 3, 5, 10, 20, 30 and 50 Hz) were made at several temperature steps (isothermally using increments of 5 °C). Data collected from these tests were used to generate master curves by employing the time–temperature superposition principle (Ferry, 1980).

2.5. Large deformation mechanical tests

Films were cut with a scalpel or scissors into strips (~50 × 8 × 0.3 mm) and after conditioning at various moisture contents they were analyzed with a TA-XT2i instrument (Stable Micro systems, Godalming, Surrey, UK) in the tensile mode operated according to ASTM D828-88 method (ASTM, 1989) at 25 °C. Cross head speed was set at 180 mm/min. The thickness of each sample was measured at three different points with a micrometer and an average value was obtained. Calculations of tensile (Young's) modulus (E), tensile strength (σ_{max}) and percentage elongation were made as described elsewhere (Arvanitoyannis & Psomiadou, 1994). The Young's modulus (E) was calculated from the initial slope of the stress–strain curves, while σ_{max} and (%) elongation correspond to the tensile strength and percentage elongation at break, respectively. Each of the reported moduli and σ_{max} values represent an average of at least eight measurements of samples similarly conditioned at a certain moisture level.

3. Results and discussion

3.1. Structural characterization of pullulan

Weight-average (M_w) and number-average (M_n) molecular weights, radius of gyration (R_g), molecular size distributions and polydispersity index were determined by a HPSEC system coupled with multiangle laser light scattering and differential refractive index detectors (HPSEC-MALLS-RI). The elution RI profiles of all samples are shown in Fig. 1, whereas estimates of their molecular characteristics (M_w, M_n, R_g, M_w/M_n) are summarized in Table 1. The eluting profiles revealed rather broad molecular size distributions. This was more pronounced with P_{360} and P_{100}, and the sample $P_{60,12}$ which showed two overlapping peaks in the smaller molecular size elution region of the chromatogram. For the high molecular size samples (P_{560} and P_{360}) a small portion of the polysaccharide was eluted in the void volume (Fig. 1). The M_w and M_n values of pullulans varied between 99–564 × 10^3 and 43–297 × 10^3, respectively, whereas the fractions in the smallest molecular size sample had M_w of 64 and 12 × 10^3, and M_n of 49 and 9 × 10^3. The R_g values also varied widely from 16 to 32 nm and did not seem to correlate with the molecular size of the samples. The M_w/M_n ratios were less than 1.9 except for the samples P_{360} and P_{100} that exhibited high polydispersity indices of 2.4 and 2.3, respectively (Table 1). The ^{13}C NMR spectral features of the samples were all typical of pullulan (data not shown); the spectra clearly pointed out to the purity of the pullulan preparations that were found essentially free of contaminating small molecular weight carbohydrates or proteins.

3.2. Solution rheology

The power of polysaccharides to influence fluid rheology arises from the greater volume the macromolecule occupies in solution compared to the total of the molecular dimensions of its repeating units. The intrinsic viscosity,

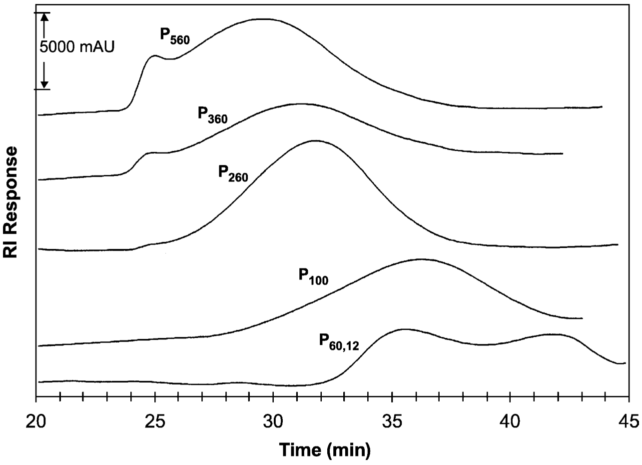

Fig. 1. HPSEC traces of pullulan preparations detected by RI.

Table 1
Molecular characteristics of pullulan samples

Sample	Molecular characteristics			
	$M_w \times 10^3$	$M_n \times 10^3$	R_g (nm)	(M_w/M_n)
P_{560}	564 ± 7.1	297 ± 1.2	30 ± 6.4	1.9 ± 0.0
P_{360}	361 ± 0.0	150 ± 0.7	32 ± 0.0	2.4 ± 0.0
P_{260}	263 ± 4.2	164 ± 0.9	26 ± 0.7	1.6 ± 0.0
P_{100}	99 ± 0.0	43 ± 0.1	25 ± 1.0	2.3 ± 0.1
$P_{60,12}$	64 ± 0.0[a]	49 ± 0.1[a]	16 ± 2.1[a]	1.3 ± 0.1[a]
	12 ± 0.7[b]	9 ± 0.0[b]	22 ± 7.1[b]	1.3 ± 0.0[b]

[a] High molecular weight fraction of sample $P_{60,12}$ (57% ratio).
[b] Low molecular weight fraction of sample $P_{60,12}$.

[η], of pullulan samples (P_{560}, P_{360}, P_{260}, and P_{100}), which reveals the volume occupied by the individual molecules in very dilute polymer solutions (hydrodynamic volume), is given in Table 2. For the pullulan samples with M_w ranging from 100 to 560×10^3 the [η] values were within the range of 0.38–0.70 dl/g. It is generally accepted that the two principal determinants of the magnitude of [η] are the chain length (i.e. molecular weight) and chain stiffness (Morris, Cutler, Ross-Murphy & Rees, 1981). Thus, the low [η] values for pullulan samples are attributed to their low molecular weight values and to the relatively high chain flexibility of pullulan originating from the α-(1 → 6) linkage which has much greater rotational freedom than other type of linkages in D-glycans. Typical values of [η] for other polysaccharides in aqueous solvents range between 0.37 and 36 dl/g (Launay, Doublier & Cuvelier, 1986).

The solution behavior of pullulan samples was examined by measuring the 'zero shear' specific viscosity $(\eta_{sp})_0$ at various concentrations (c) of the polysaccharide. The double logarithmic plots of $(\eta_{sp})_0$ against c (Fig. 2) showed a pronounced increase in viscosity gradient above a specific critical concentration (c^*). At low polymer concentrations (dilute region), $(\eta_{sp})_0$ increased approximately linearly with increasing concentration, but at higher concentrations (entangled domain) the slopes changed abruptly to much higher values. Similar behavior is well known for solutions of many typical 'random coil' polysaccharides (Morris et al., 1981), and is attributed to the transition from the dilute solution regime, where individual polymer molecules are present as isolated coils, to a concentrated solution where the total hydrodynamic volume of the individual chains exceeds the volume of the solution. Thus, c^* marks the point where the individual coils start to entangle and the onset of significant coil overlap and interpenetration. The critical concentration (c^*) depends on the volume occupied by each molecule and the differences in the value of c^* among the pullulan samples, ranging from 1.4 to 3.1 g/dl, originate essentially from molecular size differences, i.e. the value of c^* progressively increased with increasing molecular weight (M_w) of the polysaccharide (Table 2). Izydorczyk and Biliaderis (1992a) have reported a similar trend for the c^* values estimated for several wheat arabinoxylan fractions which varied in the range 0.26–0.38 g/dl. Kasapis and Morris (1994) have found that the onset of chain entanglement in solutions of a microbial capsular polysaccharide (CPS) does not occur until a comparatively high concentration (~2.0 w/v) because of its low hydrodynamic volume. Also, the c^* value depends on the structure of the polymer, which may affect its chain stiffness and, therefore, the flow characteristics. However, if $(\eta_{sp})_0$ are plotted against the (dimensionless) product of polymer concentration (proportional to the number of chains present) and intrinsic viscosity (proportional to the hydrodynamic volume of each chain), rather than against concentration alone, the data for different polysaccharides superimpose closely, regardless of polymer primary structure and molecular weight (Morris et al., 1981). Such plot, $(\eta_{sp})_0$ against $c[\eta]$, is presented in Fig. 2 (inset) for the pullulan samples and is used to determined the transition from the dilute to the concentrated regime. Master curves of log $(\eta_{sp})_0$ versus log $c[\eta]$ have been also drawn for guar gum, locust bean gum (Launay et al., 1986), and wheat arabinoxylan (Izydorczyk & Biliaderis, 1992a,b) with samples of varying molecular weight. The dimensionless coil overlap parameter ($c^*[\eta]$), a measurement of the total volume occupied by all coils within the polymer solution regardless of their molecular weight, was also estimated from these plots. The $c^*[\eta]$ values (1.0–1.2) given in Table 2 were much lower than those reported by Morris et al. (1981) for other random coil polysaccharides like dextran, carboxymethylamylose, high mannuronate alginate, and lambda carrageenan ($c^*[\eta] = 4$), but close to those for polysaccharides like amylose ($c^*[\eta] = 1$; Ellis & Ring, 1985), dextran ($c^*[\eta] = 0.8$–2.2; Sabatié et al., 1988), guar gum ($c^*[\eta] = 1.0$) or locust bean gum ($c^*[\eta] = 1.3$; Doublier & Launay, 1981). At lower degrees of coil overlap (dilute regime, $c < c^*$) the slope of double logarithmic plots of $(\eta_{sp})_0$ against $c[\eta]$ was close to 1.0 for all samples studied (Fig. 2), while at higher values (concentrated regime, $c > c^*$) the slopes increased to 2.0–2.4. For polymers of different primary structure but with similar conformational characteristics, it has been observed that the range of slope values at the dilute regime is relative narrow between 1.1 and 1.6, while at the concentrated regime the slope may take a wider range from 1.9 up to 5.6 (Lapasin & Pricl, 1999).

Table 2
Limiting viscosities, critical concentrations, coil overlap parameters, and slopes of the regression lines $\log(\eta_{sp})_0$ vs $\log c[\eta]$ in the two flow regimes for pullulan samples

Samples	[η] (dl/g)	c^* (g/dl)	($c^*[\eta]$)	Slopes	
				$c < c^*$	$c > c^*$
P_{560}	0.70	1.4	1.0	0.94	2.42
P_{360}	0.56	1.8	1.0	1.00	2.37
P_{260}	0.49	2.1	1.0	1.01	2.19
P_{100}	0.38	3.1	1.2	0.95	2.03

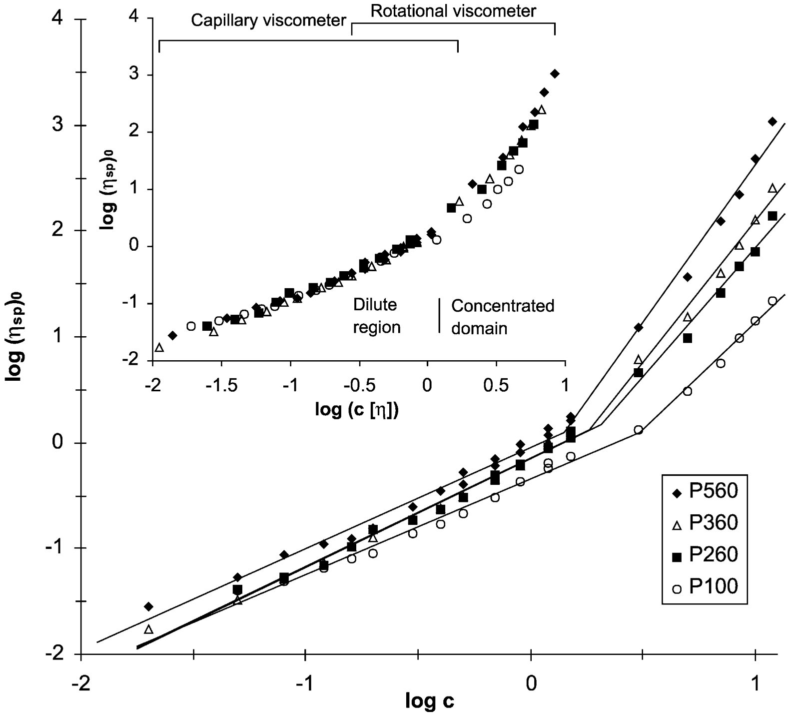

Fig. 2. Concentration dependence of zero shear spesific viscosity $(\eta_{sp})_0$ for aqueous solutions of pullulan samples. Inset: zero shear specific viscosity as a function of the overlap parameter ($c[\eta]$) for P_{560}, P_{360}, P_{260}, and P_{100} pullulan.

3.3. Thermomechanical properties of low moisture pullulan samples

The thermomechanical behavior of pullulan, either alone or with sorbitol (plasticized at a 10% d.b. level) in the glass transition zone was examined by DMTA. The effect of water on DMTA traces of a representative sample (P_{100}) is demonstrated in Fig. 3. A large drop in storage modulus E' ($\sim 10^{1.5}-10^3$ Pa) and a peak in $\tan\delta$ mark the glass transition (also denoted as α-relaxation) of the material; the $\tan\delta$ peak is normally found at a temperature higher than the onset temperature of the modulus (E') drop. The location of glass transition shifted to lower temperatures with increase of water content or addition of sorbitol due to polymer plasticization by these low molecular size compounds. The sensitivity of this transition to moisture complicates the DMTA analysis if one considers possible moisture gradients within the sample as well as moisture loss during the thermal scan, conditions which can lead to broadening of the transition. For example, with a glass transition above 80 °C (at m.c. <7% w/w) in the case of P_{100} (Fig. 3) there is an increased breadth of the $\tan\delta$ and E' drop. It is interesting also to note that the magnitude of the drop in E' and the $\tan\delta$ peak height (Figs. 3 and 4) at T_g increased significantly with increasing water content in the pullulan samples. The height of the $\tan\delta$ peak has been found to be related to the volume of the relaxing phase (Wetton, 1986) and the magnitude of the E' in the rubbery region, is related to the crosslink density or the remaining hydrogen bonding (Kalichevsky, Blanshard & Marsh, 1993). It appears that water increases the mobility of biopolymers, but may also in some way reduce self-association (by hydrogen bonding) between chains, thus reducing cross linking and increasing the volume of the relaxing phase. In this case, the reduction in rubbery modulus, and consequently the increased magnitude of E' drop, with increasing water content may be due to polymer–polymer hydrogen bonds being replaced by polymer–water hydrogen bonds. This type of mechanical behavior has also been observed in other water-plasticized biopolymers, and

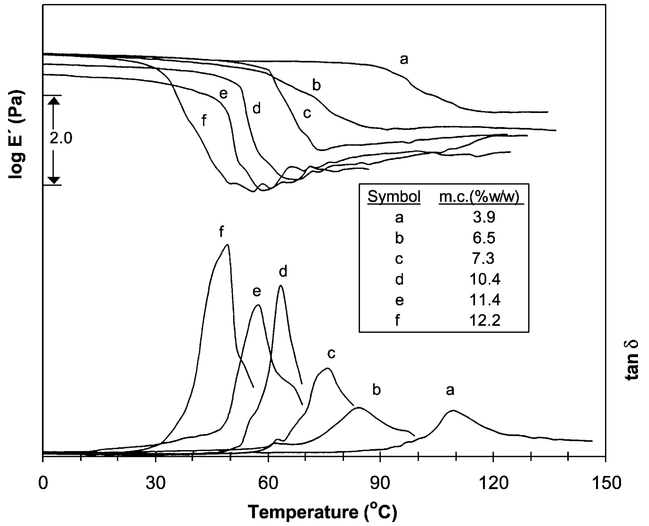

Fig. 3. DMTA log E' and $\tan\delta$ for P_{100} pullulan at different moisture content; single cantilever bending mode, heating rate 2 °C/min, frequency 3 Hz.

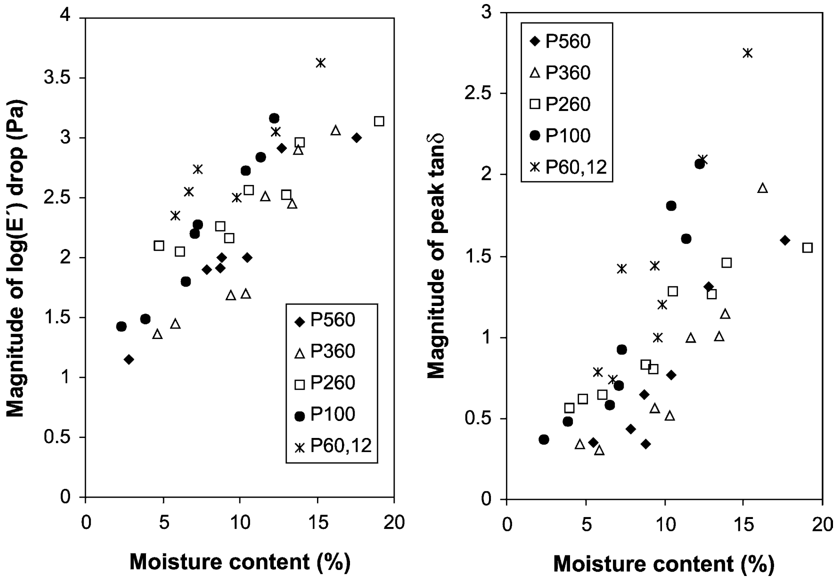

Fig. 4. Magnitude of log E' drop and peak tan δ at T_g as determined from the DMTA traces (frequency 3 Hz) of pullulan samples.

their blends, such as amylopectin (Kalichevsky, Jaroszkiewicz, Ablett, Blanshard, & Lillford, 1992a), gluten (Kalichevsky, Jaroszkiewicz, & Blanshard, 1992b), gelatinized wheat starch (Vodovotz & Chinachoti, 1996), and amylopectin–gluten blend (Kalichevsky & Blanshard, 1992). A gradual increase in E' above T_g, particularly in the wetter samples of pullulan (Fig. 3), has been also noticed which could be attributed to material stiffening due to water loss. This behavior has also been observed in hydroxypropyl cellulose films caused by crosslinking, solvent evaporation or crystallization (Rials & Glasser, 1988) and in amylopectin (Kalichevsky et al., 1992a) due to both water loss and retrogradation (recrystallization) events.

Fig. 5a shows the moisture content dependence of T_g for pullulans of varying molecular weight. The state diagrams presenting experimental DMTA data (onset of log E' drop, frequency 3 Hz) demonstrate the effect of molecular weight and water on T_g of the polysaccharide. There was no indication for an effect of T_g with molecular weight in the range of molecular mass studied. At certain moisture content the differences in T_gs among the samples were lower than 20 K within the range of water content 3–20%

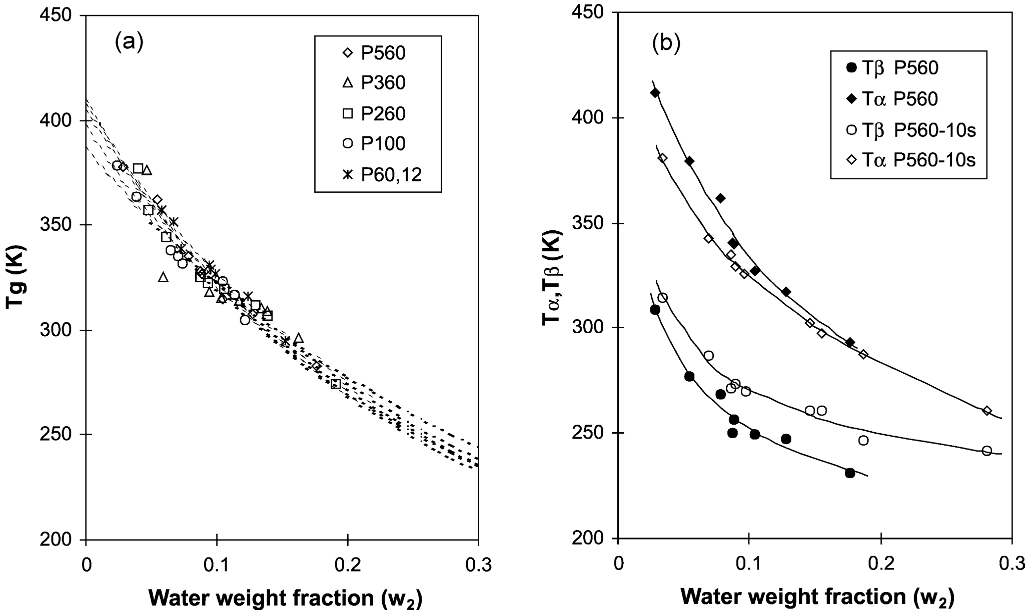

Fig. 5. (a) State diagrams of pullulan samples; dotted lines give the G–T plots of experimental data (best fit of DMTA onset of the log E' drop values at 3 Hz). (b) Temperature–water content plot for the α (T_α) and β (T_β) relaxations in a pullulan sample (P_{560}) and pullulan with 10% (d.b.) sorbitol (P_{560}-10s) as determined from the DMTA traces at 3 Hz.

(w/w). Moreover, all samples exhibited similar water plasticization responses. Modeling the T_g depression by water, using the empirical G–T equation is shown in Fig. 5a and confirmed previous observations. For a series of polysaccharides, widely differing in their molecular structure, branching, and conformation, Bizot et al. (1997) have showed that their T_gs varied only by 5–20 °C over a moisture content range of 5–25% w/w, and gave parallel trends in the T_g–moisture contents plots, implying similar plasticization responses. The glass transition temperature of linear homopolymers generally increases with increasing molecular weight (M), following a linear relationship between T_g and M^{-1} (Fox & Flory, 1950). This relationship was also found to apply to amorphous polymers of glucose (Orford, Parker, Ring, & Smith, 1989) and maltodextrins with molecular weights, however, lower than 3600 (Roos & Karel, 1991). Other studies on oligomers and amorphous polymers of amylose and cellulose derivatives (Cowie, 1975; Cowie & Henshall, 1976) further pointed out to three regimes of molecular weight dependence of T_g when plotting T_g vs $\log x$ (where x is the number of chain segments). These three domains correspond to: (i) dependent oligomeric behavior, (ii) polymeric behavior ($1/M_w$ dependence) up to the critical chain entanglement threshold, and (iii) infinite high polymer plateau. Thus, for a homologous series of amorphous linear polymers, T_g increases linearly with increasing M_n, due to decreasing free volume contributed by chain ends, up to a plateau limit where the region of entanglement coupling in the network of randomly coiled polymer chains (typically at $M_n = 1.25 \times 10^3$ to 10^5 Da) occurs, leading to a T_g level-off with further increases in M_n (Slade & Levine, 1991). Obviously, the pullulan samples examined in the present work correspond to the entanglement region of high molecular weight polymers.

The estimated parameters from the fitting of G–T equation to the experimental data, T_g of dry matrices (T_{g1}) and k constants are summarized in Table 3. Very good fits ($r^2 > 0.96$) were obtained in all cases. As it was expected, the T_{g1} of dry pullulan samples was higher (30–40 K) than the T_{g1} of the corresponding specimens with sorbitol. For a pullulan sample with certain moisture content there was a noticeable reduction in the T_g by adding sorbitol, as shown in Fig. 5b. Moreover, the plasticizing action of polyol seemed to be greater at lower levels of water content (<15% w/w). This is in agreement with the finding of Kalichevsky and Blanshard (1993) on plasticization effects of fructose and water on amylopectin. A stronger effect of fructose on the T_g of amylopectin at lower water contents was attributed by these workers to greater volume fractions of fructose in samples of reduced water content. On the other hand, because of its low molecular weight the plasticizing effect of water dominates that of fructose as the water content is increased. Similar observations have been made in a previous study on plasticization effects of sorbitol and water on chitosan, chitosan/starch and chitosan/pullulan blends (Lazaridou & Biliaderis, 2002).

Table 3
Estimated parameters of Gordon–Taylor equation using the T_g data as defined from the onset of elastic modulus (E') drop and the peak tan δ

Sample	Onset E'			Peak tan δ		
	T_{g1} (K)	k	r^2	T_{g1} (K)	k	r^2
P_{560}	408.7	4.16	0.99	450.5	5.10	0.99
P_{360}	386.3	3.03	0.96	427.9	3.64	0.99
P_{260}	404.2	3.86	0.99	415.9	3.66	0.99
P_{100}	396.6	3.73	0.99	426.3	4.09	0.99
$P_{60,12}$	406.8	3.77	0.99	426.8	3.70	0.99
P_{560}-10s	369.4	3.01	0.99	395.8	3.10	0.99
P_{360}-10s	354.6	2.50	0.99	400.8	3.20	0.99
P_{260}-10s	379.3	3.48	0.99	392.6	3.12	0.99
P_{100}-10s	371.3	3.01	0.99	386.1	2.57	0.99

A β-relaxation peak was also observed in the tan δ curve of the DMTA traces of sorbitol and/or water-plasticised pullulan samples. This transition appeared at sub-T_α temperatures and shifted to lower temperatures with increase in moisture content, as showed in Fig. 5b. In past, mechanical and dielectric spectroscopies data revealed secondary relaxations, dependent more or less on the water, for amorphous glucose and maltose (Noel, Parker, & Ring, 1996), cellulose (Montes & Cavaille, 1999; Montes et al., 1997), dextran (Bradley & Carr, 1976; Montes & Cavaille, 1999; Scandola, Ceccorulli, & Pizzoli, 1991), amylose (Bradley & Carr, 1976), chitosan (Lazaridou & Biliaderis, 2002; Ratto, Chen, & Blumstein, 1996), amorphous polymers of wood (Kelley, Rials, & Glasser, 1987), and bread (Le Meste, Roudaut, & Davidou, 1996; Roudaut, Maglione, van Dusschoten, & Le Meste, 1999a; Roudaut, Maglione, & Le Meste, 1999b). The β-relaxation in polysaccharide systems is often attributed to rotation of hydrated methylol groups or local motions of main chain segments in the disordered regions (Bradley & Carr, 1976; Montes et al., 1997). For several α-D-glucans, including pullulan, Scandola et al. (1991) detected two sub-T_α relaxations by DMTA, both sensitive to water content of the sample. The very low-temperature relaxation was attributed to small-amplitude oscillations of the sugars rings about the glycosidic linkages, whereas the second transition at much higher temperatures was interpreted as a water-induced relaxation of the polymer segments due to the plasticizing action of the solvent. In hydrated polysaccharides the formation of water–polymer bridges, causes a loosening of the H-bond network in the polymer matrix, giving higher conformational freedom to the polymer chain and thus shifting the relaxation process to lower temperatures. Such a type of relaxation in hydrophilic polysaccharides has been ascribed to diluent-induced secondary relaxations (Noel, Ring, & Whittman, 1993) and has been also detected by Diab, Biliaderis, Gerasopoulos, and Sfakiotakis (2001) for sorbitol and /or water-plasticized pullulan, using DMTA. The β-relaxation seems to be an important phenomenon in food technology, because it is connected with molecular mobility at sub-T_g temperatures (Simatos et al., 1995).

The addition of sorbitol to pullulan specimens shifted the α-relaxation to lower temperature and the β-relaxation to higher temperature, resulting in a disappearance of the low temperature relaxation, or a merger with the primary α-relaxation at high moisture contents. As shown in Fig. 5b, the β-relaxation temperature becomes progressively closer to the α-relaxation temperature with increasing water content of the pullulan–sorbitol mixture. These findings are in agreement with a recent study of Lourdin, Ring, and Colonna (1998) on maltose–glycerol and amylose–glycerol–water interactions by dielectric thermal analysis. In the two systems studied, the α-relaxation decreased when glycerol was added, but β-relaxation showed an increase. According to Lourdin et al. (1998) this effect indicates that the low temperature relaxation is probably the result of a coupling of the β motions of maltose or amylose and the α-relaxation of pure glycerol. In a advanced model developed by Ngai et al. (1988, 1991), a coupling parameter *n* between the intramolecular motions of different adjacent molecules was found proportional to the strength of the mutual dynamic constrains. Strengthening the constraints will increase *n*, and mitigating them will decrease its value. These researchers applied the coupling model to explain the antiplasticization effect of a small molecular weight substance (polychlorinated biphenyls) on the secondary relaxation of polycarbonates of Bisphenol A (BPA-PC). Polychlorinated biphenyls act as a plasticizer to the primary relaxation, facilitating the segmental mobility, but they cause an increase in the coupling parameter of the phenyl secondary relaxation in BPA-PC.

The dynamic mechanical tan δ peaks, corresponding to the α- and β-relaxations, shift to higher temperatures with increasing frequency as expected for any thermally activated relaxation process (Fig. 6a). The sensitivity of these relaxation processes to frequency permits their discrimination from other structural changes such as crystallization or melting. Plotting the frequency dependence of the two peak temperatures, the relaxation maps of Fig. 6b were obtained for pullulan at different moisture levels. Within the frequency range (1–20 Hz) used in this work the variation of log *f* with 1/*T* was linear, corresponding to an apparent Arrhenius behavior for both the α- and β-processes. The activation energy for the α-relaxation ($E_\alpha\alpha$) and β-relaxation ($E_\alpha\beta$) can be thus determined from the Arrhenius rate relationship:

$$\ln f = -(E_\alpha/RT)$$

The regression coefficients (r^2) of Arrhenius plots and the calculated activation energies ($E_\alpha\alpha$ and $E_\alpha\beta$) for some representative samples of pullulan (co-plasticized with sorbitol or not) at different moisture levels are summarized in Table 4. The activation energies varied within 171–640 kJ/mol. This range of values are in close agreement with recent findings: 300–488 kJ/mol for pullulan plasticized with sorbitol and/or water (Diab et al., 2001) and 225–545 kJ/mol for water plasticized chitosan, starch/chitosan, and pullulan/chitosan blends (Lazaridou & Biliaderis, 2002). These values are also close to those reported for synthetic polymers in the absence of plasticizer (351 kJ/mol) (Sperling, 1986) and amorphous wood components (~340 kJ/mol at 15% moisture) (Kelley et al., 1987). Over similar frequency ranges, for white bread samples with 0 and 5% moisture, $E_\alpha\alpha$ values of 424 and 370 kJ/mol, respectively, were reported (Le Meste et al., 1996), whereas in a recent study for white bread with 2% water an activation energy of 560 kJ/mol was found (Roudaut et al., 1999a). Moreover, for amylopectin with 10% moisture (Kalichevsky et al., 1992b) and gluten with 12.9% moisture (Kalichevsky, Jaroszkiewicz, & Blanshard, 1992c) apparent activation energy estimates of 300 and 242 kJ/mol were obtained. Recently, values of 296 and

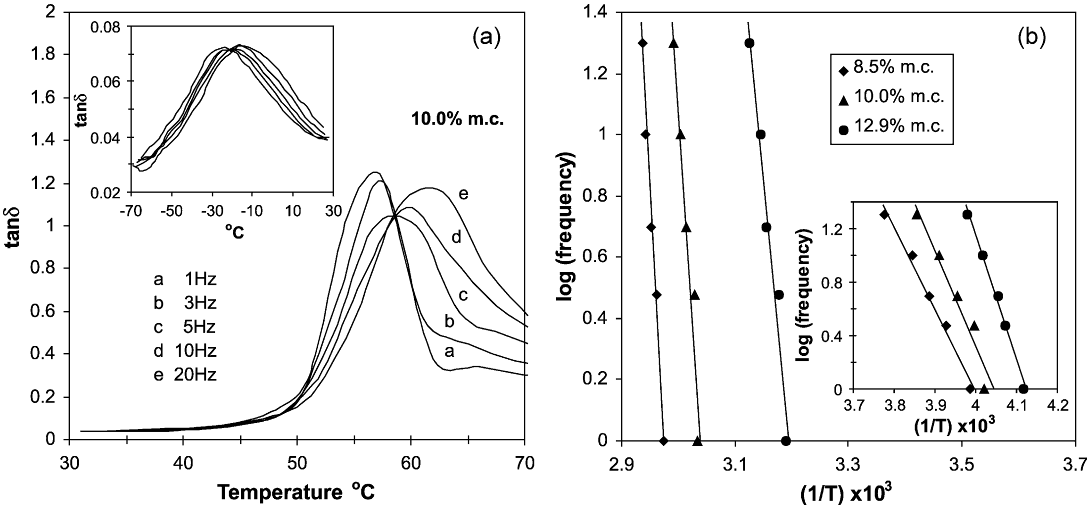

Fig. 6. Multifrequency DMTA tan δ of thermal scans (a), and Arrhenius plots of log *f* vs 1/*T* (b) for the α-relaxations and β-relaxations (insets) of P_{560} pullulan at specified moisture contents.

Table 4
Apparent activation energy (E_α) of the β and α relaxation processes and fragility parameter (*m*) estimated for pullulan samples at different moisture levels (m.c.) from Arrhenius plots applied to multifrequency DMTA data

Sample	m.c. (%w/w)	β-Relaxation		α-Relaxation		*m*
		$E_\alpha\beta$ (kJ/mol)	r^2	$E_\alpha\alpha$ (kJ/mol)	r^2	
P_{560}	8.5	118.2	0.99	640.3	0.98	95.8
P_{560}	10.0	138.9	0.94	534.0	0.95	82.9
P_{560}	12.9	179.0	0.99	360.3	0.97	59.8
P_{260}	9.1	128.2	0.96	635.4	0.89	97.4
P_{260}	10.8	130.7	0.96	506.0	0.95	80.2
P_{260}	13.1	256.2	0.98	388.7	0.97	64.2
P_{560}-10s	11.5	126.8	0.99	368.9	0.99	60.0
P_{560}-10s	14.2	–	–	279.1	0.99	47.4
P_{560}-10s	15.6	–	–	245.9	0.97	42.7
P_{260}-10s	7.6	171.5	0.98	361.0	0.98	55.5
P_{260}-10s	13.0	169.1	0.95	199.0	0.92	33.4
P_{260}-10s	15.3	–	–	170.6	0.94	29.7

226 kJ/mol for pullulan/corn starch blends plasticized (to a 20% d.b. level) with sorbitol (8.8% moisture) and xylose (13.6% moisture), respectively, have been derived from DMTA multifrequency data (Biliaderis, Lazaridou, & Arvanitoyannis, 1999). Activation energies of 200–300 kJ/mol have been reported for glass transitions in 80% sucrose solutions (MacInnes, 1993), and 240–330 kJ/mol for glucose in a moisture content range of 0–11.5% (w/w) (Noel et al., 1996). Finally, Lourdin et al. (1998) have reported an $E_\alpha\alpha$ of 128.5 kJ/mol for glycerol using dielectric analysis and Simatos et al. (1996) gave a mean $E_\alpha\alpha$ of 253 kJ/mol for sorbitol using mechanical spectroscopy data. As, it was expected, the $E_\alpha\alpha$ values showed a decrease with increasing moisture content and with the addition of sorbitol (Table 4). Moreover, pullulan alone seems to exhibit greater sensitivity in the change of $E_\alpha\alpha$ with moisture content than the corresponding samples plasticized with sorbitol. The relatively high activation energy values obtained for the α-relaxation process of many biopolymers and food systems, compared to β-relaxation, are indicative of large degrees changes in segmental mobility and a high degree of co-operativity.

The tan δ peak heights of the β-relaxations were much lower than those of the α-relaxations (Fig. 6a). The activation energies for β-relaxations varied from 118 to 256 kJ/mol (Table 4). The $E_\alpha\beta$ values for the sorbitol-plasticized samples with moisture higher than 14% (w/w) were not calculated because at these moisture levels there was a merger of the β-relaxation with the α-relaxation; as a result, the β-relaxations appeared as a shoulder of the α-relaxation and were not discerned especially at high frequencies. The estimated $E_\alpha\beta$ values were somewhat higher than those found in the literature. For dry amylose (Lourdin et al., 1998) and dextran (Montes & Cavaille, 1999) activation energies of 85 and 82 kJ/mol, respectively, have been obtained by dielectric analysis. Also, for cellulose with 0–6% (w/w) water content and for dextran with 0–9% (w/w) water $E_\alpha\beta$ of 60–85 and 48.5–83 kJ/mol, respectively, have been estimated from dynamic mechanical data (Montes et al., 1997). Moreover, $E_\alpha\beta$ values between 42 and 64 kJ/mol for glucose in the moisture content range of 0–30% (w/w) have been reported based on dielectric measurements (Chan, Pathmanathan, & Johari, 1986; Noel et al., 1996). Scandola et al. (1991) have reported $E_\alpha\beta$ of 32, 39 and 52 kJ/mol for dextran, pullulan and amylose, respectively, in the dry state. The apparently higher $E_\alpha\beta$ values found in the present study could be accounted for by differences in the technique, heating rate, frequency or temperature range used in these experiments. Dielectric measurements only detect the relative high frequency (>5 kHz) motions of dipoles, whereas dynamic mechanical data reflect rheologically important motions of chain segments (Starkweather & Avakian, 1989). For a low-moisture (<9% d.b.) white bread sample, Roudaut et al. (1999a) observed a dielectric secondary relaxation in the vinicity of −60 °C having an apparent activation energy of 50 kJ/mol. This relaxation was attributed to the rotation of the hydroxyl function present on the C_2, C_3 or C_6 of the glucosidic units. For the same product, an additional mechanical relaxation peak (water-sensitive secondary relaxation) detected at 10 °C having an apparent activation energy of 140 kJ/mol, has been ascribed to restricted motions of the main chain segments or side chains. The β-relaxation peaks of pullulan reported herein exhibit the same features (temperature, order of E_α, water sensitivity) with the mechanical secondary relaxations of white bread in the study of Roudaut et al. (1999a). Since the magnitude of E_α of these peaks was intermediate between the values usually obtained for secondary processes and those of a typical α-relaxation, some cooperative effects may also underlie these relaxation events. The $E_\alpha\beta$ values of pullulan samples in Table 4 showed a slight increase with increase of moisture content up to 10% and a larger increase with further increases in moisture. In previous studies with dextran (also assuming a random coil conformation) there was no clear trend in the $E_\alpha\beta$ values with a variation in moisture content (Montes et al., 1997). Generally, the observed changes in the $E_\alpha\beta$ values with water content were relatively small, compared to α-relaxation events, and their interpretation is not feasible with our knowledge of the origin of the β-process.

From the apparent activation energies of the α-relaxation, the fragility parameter, *m* (Angell et al., 1994), has been calculated using the following relationship:

$$m = (-E_\alpha/2.303RT_g).$$

This parameter, introduced by Angell to simplify the applicability of the concept of 'strong/fragile' glass-forming liquids, is the slope of the T_g-scaled Arrhenius plot of any relaxation time (or any property, such as viscosity, which is proportional to a relaxation time) measured at T_g (Angell et al., 1994). Strong materials are those for which the temperature coefficient for a mechanical property does not vary much with increasing temperature above T_g. In contrast, fragile materials show a strong decline in their mechanical properties above T_g and as a result a rapid degradation of their microstructure. Using the above equation, the derived E_α values for the α-relaxation from the DMTA data and the corresponding glass transition temperatures estimated from the G–T plots, the parameter *m* was calculated for the examined pullulan specimens at different moisture levels (Table 4). The estimated values of parameter *m* varied between 30 and 96. This range is close to that reported for chitosan, starch/chitosan and pullulan/chitosan blends (40–75) (Lazaridou & Biliaderis, 2002). The m values for the sorbitol-plasticized samples are in close agreement with the findings for other biopolymers: $m = 40.5 \pm 2.0$ for poly-L-asparagine (15–24% m.c.) (Angell et al., 1994); $m = 43$ for elastin (~22% m.c.) (Lillie & Gosline, 1993); $m = 40$ for gluten (~13% m.c.) (Kalichevsky et al., 1992a); $m = 51$ and $m = 42$ for pullulan/corn starch blends plasticized (to a 20% d.b. level) with sorbitol (~9% moisture) and xylose (~13.5% moisture), respectively (Biliaderis et al., 1999). Such values of m are characteristic of relative strong materials according to Angell's classification, i.e. the materials are structurally resistant when heated above their T_gs. Fragility decreased with increasing moisture content of the pullulan samples, as shown by the decreased of m in Table 4. Similar observations have been made on solutions of hydrazine and sucrose (Angell et al., 1994) and on biopolymers such as chitosan, starch/chitosan and pullulan/chitosan blends (Lazaridou & Biliaderis, 2002). Moreover, pullulan alone seems to exhibit greater sensitivity of change in *m* with moisture content than the corresponding sorbitol-plasticized samples, meaning that neat pullulan for a small change in moisture content exhibit a considerable change in the fragility parameter, which might be of importance for the mechanical stability of products made with this biopolymer. From the definition of fragility we may expect that small variations in the value of *m* among materials would result in large differences of their stability on storage for an 'equivalent' increase in temperature (T/T_g) (Simatos et al., 1995). However, as pointed out by Le Meste (1995), measurements of the dynamic behavior of glass-forming polymers in the glass transition zone should be complemented by diffusion data to derive at reliable relationships and predictions of molecular diffusivities.

The viscoelastic properties of polymers are dependent on temperature as well as time (Ferry, 1980). The effects of time can also be observed by varying the frequency of deformation applied to a polymer. It has been often demonstrated that viscoelastic data collected at one temperature (and multiple frequencies) can be superimpose upon data collected at a different temperature simply by sifting one of the curves along the time (or frequency) axis (Ferry, 1980; Williams, Landel, & Ferry, 1955), i.e. there is equivalency between time (frequency) and temperature as they both affect material properties. Fig. 7a depicts the traces

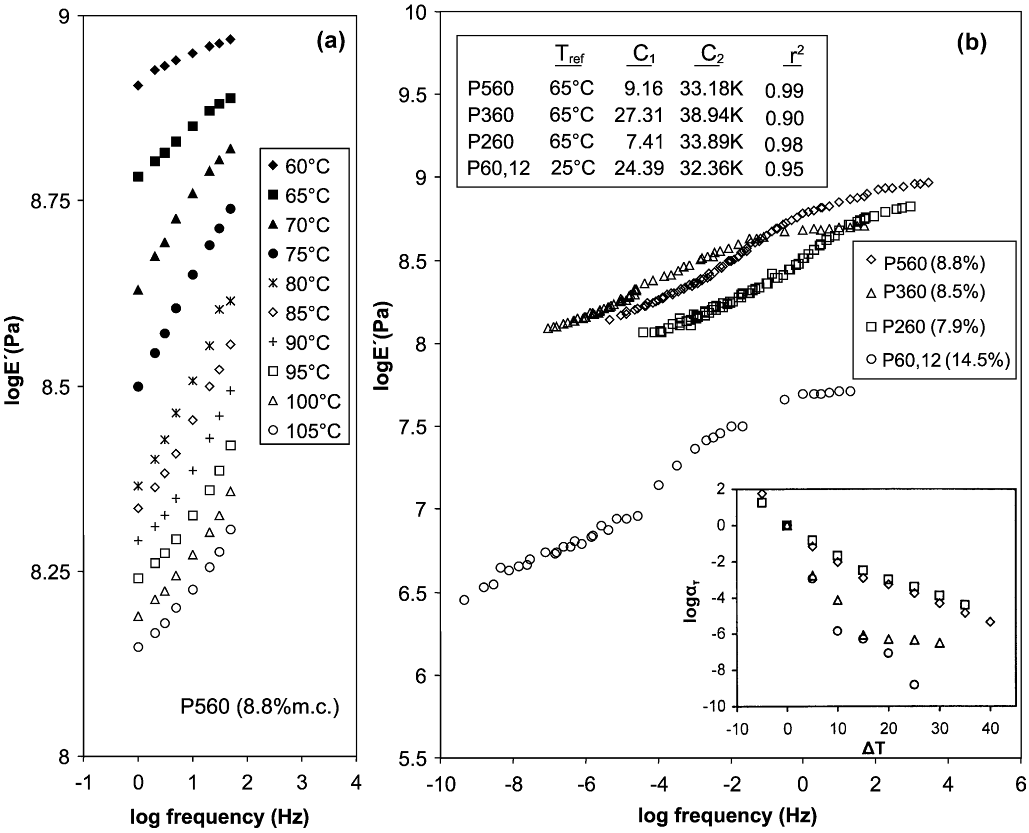

Fig. 7. Modulus–frequency curves of P_{560} pullulan (a) and master curves of log E' against frequency for pullulan samples at specified moisture contents; inset figure shows the shift factors used in the construction of the master curves against the temperature difference ($T - T_{ref}$) (b).

of storage modulus plotted logarithmically against the frequency at several temperature steps. There seemed to be little dependence of E' on frequency for temperatures below T_g; however, the modulus values did show a greater sensitivity to the applied frequency above T_g, especially in the region between T_g and ($T_g + 40$ °C). By selecting T_g as a reference temperature (taken from the onset of the log E' drop at 3 Hz), master curves were obtained, as shown in Fig. 7b. An important benefit of generating a master curve is the ability to extend the measurements in mechanical properties over a much broader frequency range or time scale, often inaccessible by practical experiments, i.e. data collected over ~2 decades of frequency can be transformed to cover ~9 orders of magnitude in our case. The degree of horizontal (time) shifting required to superimpose a given set of data with respect to a reference curve can be described by the Williams–Landel–Ferry (WLF) equation:

$$\log \alpha_T = \frac{-C_1(T - T_{ref})}{C_2 + (T - T_{ref})},$$

where α_T is the shift factor, C_1 and C_2 are constants (for many amorphous polymers they generally assume the universal values of 17.4 and 51.6, respectively), and T_{ref} is a reference temperature (e.g. T_g). This equation is typically used to describe the time/temperature behavior of polymers in the glass transition region, whereas the Arrhenius model is applied to describe the viscoelastic events associated with secondary relaxations. The WLF equation was found to be valid ($r^2 > 0.90$) over the range of T_g to ($T_g + 40$ °C); however, the derived best fit values for C_1 and C_2 differed from the universal values of the WLF constants (see Table inset in Fig. 7b). The horizontal shift factors, α_T, obtained from the generation of the E' master curves, are also plotted logarithmically in Fig. 7b (inset) against the temperature difference ΔT ($T - T_{ref}$). The α_T reflects the temperature dependence of a segmental friction coefficient or mobility on which the rates of all configurational rearrangements depend (Williams et al., 1955). The present findings are consistent with previous studies on other biopolymers where the applicability of the WLF equation has been demonstrated only over a limited range of temperatures and optimization of the C_1 and C_2 coefficients (Biliaderis et al., 1999; Kelley et al., 1987; Lazaridou & Biliaderis, 2002; Nakamura & Tobolsky, 1967).

3.4. Tensile properties and physical state of pullulan films

Fig. 8 shows the effect of molecular weight on the force–distance (or stress–strain) curves of pullulan at specified moisture contents (~13–15% w/w), obtained by tensile tests. At this moisture content range, with decreasing molecular weight, the maximum force at break and the slope of the curve decreased, reflecting the gradual transition of the material from brittle to ductile failure. A very strong dependence of the slope of the deformation curves on molecular weight has been noticed for many synthetic polymers by tensile tests; the slope as well as the fracture stress at break increase with increasing molecular weight of the polymer (Ito, Takahashi, Araki, & Kanamoto, 2001; Jordens, Wilkes, Janzen, Rohlfing, & Welch, 2000; Kennedy, Peacock, Failla, Lucas, & Mandelkern, 1995; Kennedy, Peacock, & Mandelkern, 1994; Niesten & Gaymans, 2001).

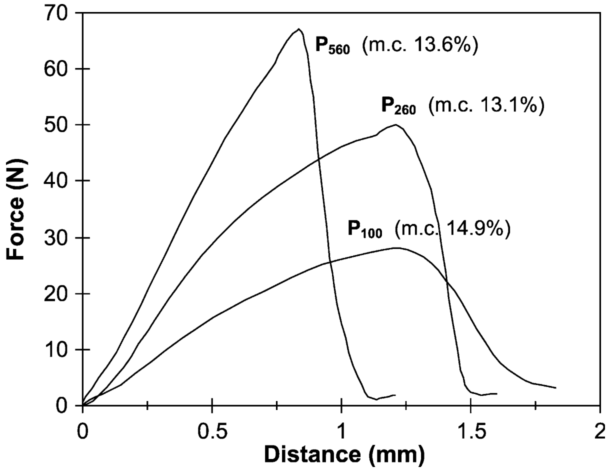

Fig. 8. Load–deformation curves (tensile tests) for pullulan with different molecular weights at specified moisture contents.

Figs. 9 and 10 show the effect of varying moisture content, molecular weight and addition of sorbitol on the mechanical properties of pullulan films, as calculated from the stress–strain curves and described by the tensile modulus (E), tensile strength (σ_{max}) and percentage elongation. In general, at moisture contents less than 7–10%, films exhibited high tensile modulus, high tensile strength, and low elongation values, at room temperature, typical of glassy materials. With increasing water content there was a gradual transition from brittle to ductile failure for all the films, typical of polymers going through their glass transition. This state transition is accompanied by sharp decreases in modulus and tensile strength, and an increase in elongation as shown in Figs. 9 and 10. With addition of sorbitol (10% d.b.) there was a decrease in modulus and tensile strength, whereas the percentage elongation showed a substantial increase from ~10 to 50–300%. Also, adding the polyol made sharper the fall in E and σ_{max} with increasing water content (Fig. 10). The effects of water and sorbitol on the mechanical properties of pullulan films can be attributed to their plasticizing properties, as has been shown in previous studies for pullulan films (Diab et al., 2001), pullulan-based blends (Biliaderis et al., 1999; Lazaridou & Biliaderis, 2002) and many other biopolymers (Bader & Goritz, 1994; Fontanet, Davidou, Dacremont, & Le Meste, 1997; Kirby, Clark, Parker, & Smith, 1993; Lawton, 1996; Le Meste et al., 1996; Park and Ruckenstein, 2001; Park, Weller, Vergano, & Testin, 1993; Van Soest, Benes, & Wit, 1996a; Van Soest, Wit, & Vliegenthart, 1996b). The observed range of σ_{max} values (10–80 MPa) is similar to the tensile strength (10–90 MPa)

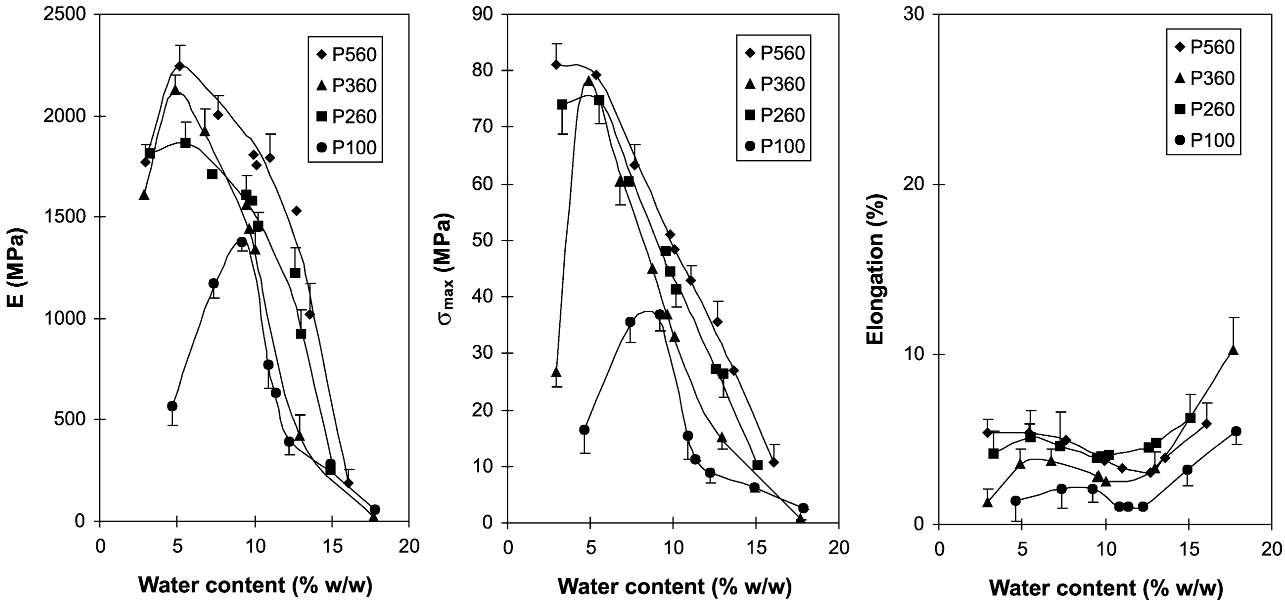

Fig. 9. Effect of water content on tensile modulus, tensile strength and percentage elongation as determined from tensile tests of pullulan with different molecular weights; points are means of at least eight measurements and half-bars show the standard deviation values.

values reported for pullulan (Diab et al., 2001) and composite pullulan/chitosan (Lazaridou & Biliaderis, 2002) films. Shih (1996) has found a comparable tensile strength value (~35 MPa) for pullulan films, after exposure to 65% relative humidity for 48 h.

For most pullulan films a bell-shape curve, describing the relationship between the tensile parameters (E, σ_{max}) and moisture was found (Figs. 9 and 10). Such a behavior has been previously reported for mechanical parameters of foods and their components (Attenburrow, Davies, Goodband, & Ingman, 1992; Biliaderis et al., 1999; Diab et al., 2001; Fontanet et al., 1997; Harris & Peleg, 1996; Lazaridou & Biliaderis, 2002; Nicholls, Appelqvist, Davies, Ingman, & Lillford, 1995). The most striking feature of these plots is the apparent increase in stiffness as the moisture rises from 3 to 7%, whereas the softening/plasticizing effect of water becomes dominant above this level. Several suggestions have been made to explain such material toughening on partial plasticization with water. According to Harris and Peleg (1996), glassy biopolymers at low moisture are extremely brittle and very fragile, offering no resistance to applied load. With low levels of hydration, the plasticised matrix becomes more cohesive, more structural elements remain intact (offering more resistance to fracture), and the

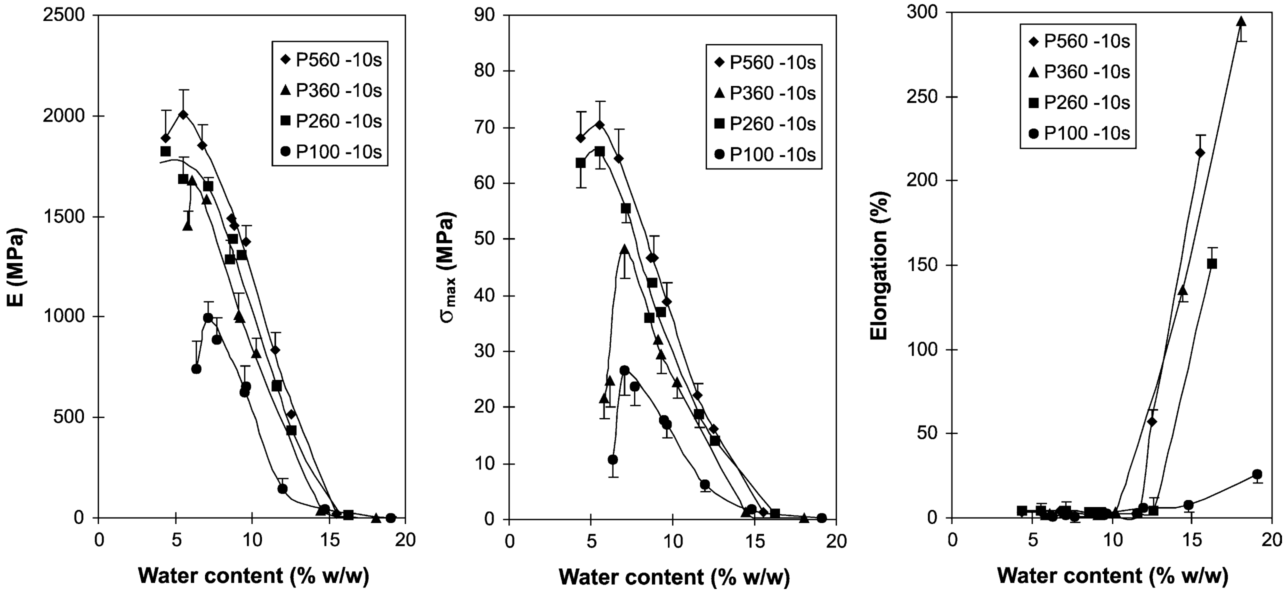

Fig. 10. Effect of water content on tensile modulus, tensile strength and percentage elongation as determined from tensile tests of sorbitol-plasticized pullulan with different molecular weights; points are means of at least eight measurements and half-bars show the standard deviation values.

material would deform rather than disintegrate on compression. For extruded flat bread, Fontanet et al. (1997) have ascribed the hardening phenomenon to short range reorganization of the material as a result of increased molecular mobility by adding small amounts of water. These authors have also provided an alternative hypothesis, attributing material toughening to formation of micro-shear bands caused by slight increase in free-volume during compression testing.

The tensile tests for films made with pullulan samples varying in molecular weight (P_{560}, P_{360}, P_{260}, and P_{100}) revealed that tensile modulus and tensile strength are affected by the molecular size of the polymer (Figs. 9 and 10). The lowest molecular weight pullulan material ($P_{60,12}$) could not be tested in the texture analyzer due to its extreme brittleness. The general trend was an increase of E, $\sigma_{\max}$, and elongation values with increasing molecular weight. Similarly, for several synthetic polymers the fracture stresses and strains have been found to increase with molecular weight (Ito et al., 2001; Jordens et al., 2000; Niesten & Gaymans, 2001), whereas Kennedy et al. (1994, 1995) found maximum tensile strength values at intermediate molecular weights. Similar observations have been made for biopolymers. For methyl cellulose and hydroxypropyl cellulose, Park et al. (1993) have shown an increase of tensile strength and elongation as molecular weight of the cellulose increased, whereas for thermoplastic starch Van Soest et al. (1996a) have reported an increase of elongation with molecular weight, but no significant influence on tensile modulus and tensile strength. A possible mechanism for increasing the apparent modulus with molecular weight has been suggested by Kennedy et al. (1994, 1995). Focusing on the interlamellar (amorphous) region of linear polymers, these researchers ascribed this behavior to the increased number of chain entanglements per molecule with increasing chain length; as a disordered chain moves or slips through the impediment of entanglements, its apparent modulus will increase with molecular weight. Van Soest et al. (1996a) examined two different molecular weight grades of extruded thermoplastic starch and found higher elongation values in the rubbery state for the sample with the higher molecular weight. A closer examination of the data for the tensile parameters of Figs. 9 and 10 revealed a relation of E and $\sigma_{\max}$ to the number-average molecular weight (M_n) rather than to weight-average molecular weight (M_w) (Table 1), particularly for the sorbitol-plasticized samples (Fig. 10). Thus, for P_{360} the brittle–ductile transition occurred at lower moisture content than expected on the basis of its M_w. The only difference between P_{360} and the other two high molecular weight samples of pullulan (P_{560}, P_{260}) was the high polydispersity index of the former (2.4) compared to those of P_{560} (1.9) and P_{260} (1.6). The high polydispersity of P_{360} might be responsible for the much higher elongation values obtained for this sample compared to P_{560} and P_{260} (Figs. 9 and 10). Similarly, Van Soest (1996) has found that tensile stress and modulus of thermoplastic starch decreased with increasing of molecular mass distribution, whereas the elongation increased slightly. Differences in tensile behavior among pullulan samples could be thus ascribed to a combination of molecular features such as polydispersity and molecular weight.

4. Conclusions

The molecular characteristics seem to largely influence solution rheology and the mechanical properties of pullulan under uniaxial load, whereas they seem to have very little impact on the thermomechanical properties (e.g. T_g and related relaxation processes) as probed by small deformation dynamic tests. For several linear polyethylene homopolymers of varying molecular weight, Jordens et al. (2000) have also shown very little dependence of small-strain tensile deformation properties on molecular weight, whereas the large-strain deformation behavior was significantly affected by the molecular weight of the polymer. The results of the present study suggest that both molecular size and molecular size distribution have an impact on the mechanical behavior of pullulan subjected to large deformation mechanical testing. Water and sorbitol exerted strong plasticizing effects, affecting both the α- and β-relaxation processes of the amorphous polymer phase as well as the tensile properties of the pullulan films.

Acknowledgements

The authors wish to thank Dr M. Izydorczyk from the Canadian Grain Research Commission for conducting the light scattering measurements.

References

Angell, C., Bressel, R. D., Green, J. L., Kanno, H., Oguni, M., & Sare, E. J. (1994). Liquid fragility and the glass transition. *Journal of Food Engineering*, *22*, 115–142.

Arvanitoyannis, I., & Psomiadou, E. (1994). Composites of anionic copolyamides (nylon6/nylon12) with short E-glass fibers: Preparation and properties. *Journal of Applied Polymer Science*, *51*, 1863–1899.

ASTM (1989). *Annual book of ASTM standards, D828-88*. Philadelphia: American Society for Testing and Materials.

Attenburrow, G. E., Davies, A. P., Goodband, R. M., & Ingman, S. J. (1992). The fracture behaviour of starch and gluten in the glassy state. *Journal of Cereal Science*, *16*, 1–12.

Bader, H. G., & Goritz, D. (1994). Investigations on high amylose corn starch films. *Starch*, *46*, 435–439.

Banker, G. S. (1966). Film coating theory and practice. *Journal of Pharmacy*, *55*, 81–89.

Biliaderis, C. G., Lazaridou, A., & Arvanitoyannis, I. (1999). Glass transition and physical properties of polyol-plasticised pullulan–starch blends at low moisture. *Carbohydrate Polymers*, *40*, 29–47.

Bizot, H., Le Bail, P., Lexour, B., Davy, J., Roger, P., & Buleon, A. (1997). Calorimetric evaluation of the glass transition in hydrated, linear and branched polyanhydroglucose compounds. *Carbohydrate Polymers*, *32*, 33–50.

Bradley, S. A., & Carr, S. H. (1976). Mechanical loss processes in polysaccharides. *Journal of Polymer Science. Polymer Physics Edition*, *14*, 111–124.

Chan, R. K., Pathmanathan, K., & Johari, G. P. (1986). Dielectric relaxations in the liquid and glassy states of glucose and its water mixtures. *Journal of Physical Chemistry*, *90*, 6358–6362.

Chronakis, I. S., & Kasapis, S. (1995). Food applications of biopolymers—Theory and practice. In G. Charalambous (Ed.), *Food flavors: Generation, analysis and process influence* (pp. 75–109). Amsterdam: Elsevier.

Cowie, J. M. G. (1975). Some general features of T_g–M relations for oligomers and amorphous polymers. *European Polymer Journal*, *11*, 297–300.

Cowie, J. M. G., & Henshall, S. A. E. (1976). The influence of chain length and branching on the glass transition temperature of some polyglucosans. *European Polymer Journal*, *12*, 215–218.

Deshpande, M. S., Rale, V. B., & Lynch, J. M. (1992). Aureobasidium pullulans in applied microbiology: A status report. *Enzyme and Microbial Technology*, *14*, 514–527.

Diab, T., Biliaderis, C. G., Gerasopoulos, D., & Sfakiotakis, E. (2001). Physicochemical properties and application of pullulan edible films and coatings in fruit preservation. *Journal of the Science of Food and Agriculture*, *81*, 998–1000.

Doublier, J. L., & Launay, B. (1981). Rheology of galactomannan solutions: Comparative study of guar gum and locust bean gum. *Journal of Texture Studies*, *12*, 151–172.

Ellis, H. S., & Ring, S. G. (1985). A study of some factors influencing amylose gelation. *Carbohydrate Polymers*, *5*, 201–214.

Ferry, J. D. (1980). *Viscoelastic properties of polymers* (3rd ed). New York: Wiley.

Fontanet, I., Davidou, S., Dacremont, C., & Le Meste, M. (1997). Effect of water on the mechanical behaviour of the extruded flat bread. *Journal of Cereal Science*, *25*, 303–311.

Fox, T. G., & Flory, P. J. (1950). Second-order transition temperatures and related properties of polystyrene. I. Influence of molecular weight. *Journal of Applied Physics*, *21*, 581–591.

Gordon, M., & Taylor, J. S. (1952). Ideal copolymers and the second-order transitions of synthetic rubbers. I. Non-crystalline copolymers. *Journal of Applied Chemistry*, *2*, 493–500.

Hannigan, K. (1984). Edible plastic. *Food Engineering*, *56*, 98–99.

Harris, M., & Peleg, M. (1996). Patterns of textural changes in brittle cellular cereal foods caused by moisture sorption. *Cereal Chemistry*, *73*, 225–231.

Ito, M., Takahashi, A., Araki, N., & Kanamoto, T. (2001). Effects of molecular weight on the drawing and the draw efficiency of nylon-6. *Polymer*, *42*, 241–248.

Izydorczyk, M. S., & Biliaderis, C. G. (1992a). Influence of structure on the physicochemical properties of wheat arabinoxylan. *Carbohydrate Polymers*, *17*, 237–247.

Izydorczyk, M. S., & Biliaderis, C. G. (1992b). Effect of molecular size on physical properties of wheat arabinoxylan. *Journal of Agricultural and Food Chemistry*, *40*, 561–568.

Jordens, K., Wilkes, G. L., Janzen, J., Rohlfing, D. C., & Welch, M. B. (2000). The influence of molecular weight and thermal history on the thermal, rheological, and mechanical properties of metallocene-catalyzed linear polyethylenes. *Polymer*, *41*, 7175–7192.

Kalichevsky, M. T., & Blanshard, J. M. V. (1992). A study of the effect of water on the glass transition of 1:1 mixtures of amylopectin, casein and gluten using DSC and DMTA. *Carbohydrate Polymers*, *19*, 271–278.

Kalichevsky, M. T., & Blanshard, J. M. V. (1993). The effect of fructose and water on the glass transition of amylopectin. *Carbohydrate Polymers*, *20*, 107–113.

Kalichevsky, M. T., Blanshard, J. M. V., & Marsh, R. D. L. (1993). Applications of mechanical spectroscopy to the study of glassy biopolymers and related systems. In J. M. V. Blanshard, & P. J. Lillford (Eds.), *The glassy state in foods* (pp. 133–156). Loughborough: Nottingham University Press.

Kalichevsky, M. T., Jaroszkiewicz, E. M., Ablett, S., Blanshard, J. M. V., & Lillford, P. J. (1992a). The glass transition of amylopectin measured by DSC, DMTA and NMR. *Carbohydrate Polymers*, *18*, 77–88.

Kalichevsky, M. T., Jaroszkiewicz, E. M., & Blanshard, J. M. V. (1992b). The glass transition of gluten. 2: The effect of lipids and emulsifiers. *International Journal of Biological Macromolecules*, *14*, 267–273.

Kalichevsky, M. T., Jaroszkiewicz, E. M., & Blanshard, J. M. V. (1992c). Glass transition of gluten. 1: Gluten–sugar mixtures. *International Journal of Biological Macromolecules*, *14*, 257–266.

Kasapis, S., & Morris, E. R. (1994). Solution properties of levan polysaccharide from *Pseudomonas syringae* pv. *Phaseolicola* and its possible primary role as a blocker of recognition during pathogenesis. *Carbohydrate Polymers*, *23*, 55–64.

Kelley, S. S., Rials, T. G., & Glasser, W. G. (1987). Relaxation behavior of the amorphous components of wood. *Journal of Materials Science*, *22*, 617–624.

Kennedy, M. A., Peacock, A. J., Failla, M. D., Lucas, J. C., & Mandelkern, L. (1995). Tensile properties of crystalline polymers: Random copolymers of ethylene. *Macromolecules*, *28*, 1407–1421.

Kennedy, M. A., Peacock, A. J., & Mandelkern, L. (1994). Tensile properties of crystalline polymers: Linear polyethylene. *Macromolecules*, *27*, 5297–5310.

Kirby, A. R., Clark, S. A., Parker, R., & Smith, A. C. (1993). The deformation and failure behaviour of wheat starch plasticized with water and polyols. *Journal of Materials Science*, *28*, 5937–5942.

Lapasin, R., & Pricl, S. (1999). *Rheology of industrial polysaccharides: Theory and applications*. Gaithersburg, MD: Aspen Publishers.

Launay, B., Doublier, J. L., & Cuvelier, G. (1986). Flow properties of aqueous solutions and dispersions of polysaccharides. In J. R. Mitchell, & D. A. Ledward (Eds.), *Functional properties of food macromolecules* (pp. 1–78). London: Elsevier Applied Science.

Lawton, J. W. (1996). Effect of starch type on the properties of starch containing films. *Carbohydrate Polymers*, *29*, 203–208.

Lazaridou, A., & Biliaderis, C. G. (2002). Thermophysical properties of chitosan, chitosan–starch and chitosan–pullulan films near the glass transition. *Carbohydrate Polymers*, *48*, 179–190.

Lazaridou, A., Roukas, T., Biliaderis, C. G., & Vaikousi, H. (2002). Influence of agitation on production and molecular characteristics of pullulan by *Aureobasidium pullulans* fermentation of beet molasses in a stirred tank fermentor. *Enzyme and Microbial Technology*, *31*, 122–132.

Le Meste, M. (1995). Mobility of small molecules in low and intermediate moisture foods. In V. Barbosa-Canovas, & L. Welti-Chanes (Eds.), *Food preservation by moisture control* (pp. 209–225). Lancaster: Technomic Publishing Company.

Le Meste, M., Roudaut, G., & Davidou, S. (1996). Thermomechanical properties of glassy cereal foods. *Journal of Thermal Analysis*, *47*, 1361–1375.

Lillie, M. A., & Gosline, J. M. (1993). The effects of swelling solvents on the glass transition in elastic and other proteins. In M. V. Blanshard, & P. J. Lillford (Eds.), *The glassy state in foods* (pp. 281–301). Loughborough: Nottingham University Press.

Lourdin, D., Ring, S. G., & Colonna, P. (1998). Study of plasticizer–oligomer and plasticizer–polymer interactions by dielectric analysis: Maltose–glycerol and amylose–glycerol–water systems. *Carbohydrate Research*, *306*, 551–558.

MacInnes, W. M. (1993). Dynamic mechanical thermal analysis of sucrose solutions. In J. M. V. Blanshard, & P. J. Lillford (Eds.), *The glassy state in foods* (pp. 223–248). Loughborough: Nottingham University Press.

Montes, H., & Cavaille, J. Y. (1999). Secondary dielectric relaxations in dried amorphous cellulose and dextran. *Polymer*, *40*, 2649–2657.

Montes, H., Mazeau, K., & Cavaille, J. Y. (1997). Secondary mechanical relaxations in amorphous cellulose. *Macromolecules*, *30*, 6977–6984.

Morris, E. R., Cutler, A. N., Ross-Murphy, S. B., & Rees, D. A. (1981). Concentration and shear rate dependence of viscosity in random coil polysaccharide solutions. *Carbohydrate Polymers*, *1*, 5–21.

Nakamura, S., & Tobolsky, A. V. (1967). Viscoelastic properties of plasticized amylose films. *Journal of Applied Polymer Science*, *11*, 1371–1386.

Ngai, K. L., Rendell, R. W., & Yee, A. F. (1988). Local molecular motions in glassy and dissolved polycarbonates. *Macromolecules*, *21*, 3396–3401.

Ngai, K. L., Rendell, R. W., Yee, A. F., & Plazek, D. J. (1991). Antiplasticization effects on a secondary relaxation in plasticized glassy polycarbonates. *Macromolecules*, *24*, 61–67.

Ngai, K. L., Roland, C. M., O'Reilly, J. M., & Sedita, J. S. (1992). Trends in the temperature dependency of segmental relaxation in TMPC/PC blends. *Macromolecules*, *25*, 3906–3909.

Nicholls, R. J., Appelqvist, I. A. M., Davies, A. P., Ingman, S. J., & Lillford, P. J. (1995). Glass transitions and the fracture behaviour of gluten and starches within the glassy state. *Journal of Cereal Science*, *21*, 25–36.

Niesten, M. C. E. J., & Gaymans, R. J. (2001). Tensile and elastic properties of segmented copolyetheresteramides with uniform aramid units. *Polymer*, *42*, 6199–6207.

Noel, T. R., Parker, R., & Ring, S. G. (1996). A comparative study of the dielectric relaxation behavior of glucose, maltose, and their mixtures with water in the liquid and glassy states. *Carbohydrate Research*, *282*, 193–206.

Noel, T. R., Ring, S. G., & Whittman, M. A. (1993). Relaxations in supercooled carbohydrate liquids. In J. M. V. Blanshard, & P. J. Lillford (Eds.), *The glassy state in foods* (pp. 173–188). Loughborough: Nottingham University Press.

Orford, P. D., Parker, R., Ring, S. G., & Smith, A. C. (1989). Effect of water as a diluent on the glass transition behavior of malto-oligosaccharides, amylose and amylopectin. *International Journal of Biological. Macromolecules*, *11*, 91–96.

Park, J. S., & Ruckenstein, E. (2001). Viscoelastic properties of plasticized methylcellulose and chemically crosslinked methycellulose. *Carbohydrate Polymers*, *46*, 373–381.

Park, H. J., Weller, C. L., Vergano, P. J., & Testin, R. F. (1993). Permeability and mechanical properties of cellulose-based films. *Journal of Food Science*, *58*, 1361–1364. see also page 1370.

Plazek, D. J., & Ngai, K. L. (1991). Correlation of polymer segmental chain dynamics with temperature-dependent time-scale shifts. *Macromolecules*, *24*, 1222–1224.

Ratto, J. A., Chen, C. C., & Blumstein, R. B. (1996). Phase behavior study of chitosan/polyamide blends. *Journal of Applied Polymer Science*, *59*, 1451–1461.

Rees, D. A. (1977). *Polysaccharide shapes*. London: Chapman & Hall.

Rials, T. G., & Glasser, W. G. (1988). Thermal and dynamic mechanical properties of hydroxypropyl cellulose films. *Journal of Applied Polymer Science*, *35*, 749–758.

Roos, Y., & Karel, M. (1991). Phase transitions of mixtures of amorphous polysaccharides and sugars. *Biotechnology Progress*, *7*, 49–53.

Roudaut, G., Maglione, M., van Dusschoten, D., & Le Meste, M. (1999a). Molecular mobility in glassy bread: A multispectroscopy approach. *Cereal Chemestry*, *76*, 70–77.

Roudaut, G., Maglione, M., & Le Meste, M. (1999b). Relaxations below glass transition temperature in bread and its components. *Cereal Chemestry*, *76*, 78–81.

Sabatié, J., Choplin, L., Doublier, J. L., Arul, J., Paul, F., & Monsan, P. (1988). Rheology of native dextrans in relation to their primary structure. *Carbohydrate Polymers*, *9*, 287–299.

Scandola, M., Ceccorulli, G., & Pizzoli, M. (1991). Molecular motions of polysaccharides in the solid state: Dextran, pullulan and amylose. *International Journal of Biological Macromolecules*, *13*, 254–260.

Selim, K., Tsimidou, M., & Biliaderis, C. G. (2000). Kinetic studies of degradation of saffron carotenoids encapsulated in amorphous polymer matrices. *Food Chemestry*, *71*, 199–206.

Serris, G. S., & Biliaderis, C. G. (2001). Degradation kinetics of beetroot pigment encapsulated in polymeric matrices. *Journal of the Science of Food and Agriculture*, *81*, 988–1000.

Shih, F. F. (1996). Edible films from rice protein concentrate and pullulan. *Cereal Chemestry*, *73*, 406–409.

Simatos, D., Blond, G., & Perez, J. (1995). Basic physical aspects of glass transition. In V. Barbosa-Canovas, & L. Welti-Chanes (Eds.), *Food preservation by moisture control* (pp. 3–31). Lancaster: Technomic Publishing Company.

Simatos, D., Blond, G., Roudaut, G., Champion, D., Perez, J., & Faivre, A. L. (1996). Influence of heating and cooling rates on the glass transition temperature and the fragility parameter of sorbitol and fructose as measured by DSC. *Journal of Thermal Analysis*, *47*, 1419–1436.

Slade, L., & Levine, H. (1991). Beyond water activity: Recent advances based on an alternative approach to the assessment of food quality and safety. *Critical Reviews in Food Science and Nutrition*, *30*, 115–360.

Slade, L., & Levine, H. (1993). The glassy state phenomenon in food molecules. In J. M. V. Blanshard, & P. J. Lillford (Eds.), *The glassy state in foods* (pp. 35–101). Loughborough: Nottingham University Press.

Sperling, L. H. (1986). *Introduction to physical polymer science*. New York: Wiley.

Starkweather, H. W., & Avakian, P. (1989). β Relaxations in phenylene polymers. *Macromolecules*, *22*, 4060–4062.

Sugisaki, M., Suga, H., & Seki, S. (1968). Calorimetric study of the glassy state. IV. Heat capacities of glassy water and cubic ice. *Bulletin Chemical Society of Japan*, *41*, 2591–2599.

Van Soest, J. J. G (1996). *Starch plastics, structure property relationships*. PhD Thesis, University of Wageningen, Holland.

Van Soest, J. J. G., Benes, K., & De Wit, D. (1996a). The influence of starch molecular mass on the properties of extruded thermoplastic starch. *Polymer*, *37*, 3543–3552.

Van Soest, J. J. G., De Wit, D., & Vliegenthart, J. F. G. (1996b). Mechanical properties of thermoplastic waxy maize starch. *Journal of Applied Polymer Science*, *61*, 1927–1937.

Verghese, K. N. E., Jensen, R. E., Lesko, J. J., & Ward, T. C. (2001). Effects of molecular relaxation behavior on sized carbon fiber–vinyl ester matrix composite properties. *Polymer*, *42*, 1633–1645.

Vodovotz, Y., & Chinachoti, P. (1996). Thermal transitions in gelatinized wheat starch at different moisture contents by dynamic mechanical analysis. *Journal of Food Science*, *61*, 932–937. see also page 941.

Wetton, R. E. (1986). Dynamic mechanical thermal analysis of polymers and related systems. In J. V. Dawkins (Ed.), *Developments in polymer characterization* (pp. 179–221). London: Elsevier Applied Science.

Williams, M. L., Landel, R. F., & Ferry, J. D. (1955). The temperature dependence of relaxation mechanisms in amorphous polymers and other glass-forming liquids. *Journal of the American Chemical Society*, *77*, 3701–3707.

Yuen, S. (1974). Pullulan and its applications. *Process Biochemistry*, *9*(7–9), 22.